Unresolved γ Rays in ^{114}Te: Mass Dependence of Rotational Damping

S. Frattini, A. Bracco, S. Leoni, F. Camera, B. Million, N. Blasi, G. Lo Bianco, M. Pignanelli, and E. Vigezzi
Dipartimento di Fisica, Universitá di Milano, and INFN sez. Milano, via Celoria 16, 20133 Milano, Italy

B. Herskind, T. Døssing, M. Bergström, P. Varmette, and S. Törmänen
The Niels Bohr Institute, Copenhagen, Denmark

A. Maj and M. Kmiecik
The Henryk Niewodniczański Institute of Nuclear Physics, 31-342 Kraków, Poland

D. R. Napoli
INFN, Laboratori Nazionali di Legnaro, Legnaro, Italy

M. Matsuo
Yukawa Institute of Physics, Kyoto, Japan
(Received 20 May 1999)

Unresolved γ rays of ^{114}Te sorted into one- and two-dimensional spectra were studied. The reaction ^{64}Ni($E_{\text{beam}} = 230-270$ MeV) + ^{54}Cr was used and the γ rays were detected with the EUROBALL array. The effective moment of inertia for the quasicontinuum was found to be almost constant for $I = (20-40)\hbar$, in contrast with the decreasing behavior of the terminating yrast band. A comparative analysis with the nucleus ^{164}Yb is presented and the results from a fluctuation analysis were compared with cranked shell model calculations. The comparison shows consistency in the scaling of the rotational damping width with mass number.

PACS numbers: 21.10.Re, 21.60.Ka, 23.20.Lv, 27.60.+j

The understanding of rotational motion in thermally excited nuclei is one of the central issues in nuclear structure and more in general in the study of effects beyond mean field. Until now, convincing evidence of collective damped rotation has been obtained for the mass region $A \approx 160$. The overall features of quasicontinuum spectra have been well described with the rotational damping model calculations in which the mean-field rotational bands of the cranked shell model are mixed by the residual two-body interaction [1]. In the original formulation of rotational damping [2], schematic estimates for the scaling of the mixing process of mean-field bands with mass number were derived. The energy U_0 relative to the yrast line, at which the damping (mixing) sets in, depends on the level density and on the strength of the residual interaction, and is predicted to vary with mass number $U_0 \propto A^{-2/3}$. The rotational damping width Γ_{rot}, expressing the width of the quadrupole transition strength distribution, is proportional to the statistical dispersion of the rotational frequency of cranked shell model n-particle–n-hole states. For Γ_{rot} the scaling is expected to follow the relation $\Gamma_{\text{rot}} \propto IA^{-5/2}\epsilon^{-1}$, where I, A, and ϵ are the spin, mass number, and deformation, respectively. Experiments have earlier confirmed the prediction of $U_0 \approx 0.7$ MeV for the onset of damping in rare-earth nuclei [3]. However, the damping width Γ_{rot} appears to be a quantity not easily accessible in experiments [4]. Experimentally, its variation with mass number for normally deformed nuclei has never been investigated. On the other hand, a detailed test of effects beyond mean field such as the rotational damping mechanism is also relevant in view of the analogy discussed in Ref. [5] with nuclear magnetic resonance. To determine the validity of the relation given above, one needs to compare nuclei with a similar deformation, but with different masses; good examples are nuclei with $A \approx 160$ and $A \approx 110$ for which a factor of 2 difference in the damping width is expected.

Some evidence of collective rotation in the quasicontinuum in nuclei with $A = 110-120$, characterized by spherical shapes at low spins, was found two decades ago in experiments made with scintillator detectors [6]. More recent discrete spectroscopy studies made with multigermanium detector arrays have identified discrete rotational bands at high spins for several nuclei in the $A = 110-120$ mass region. We have chosen to study the nucleus ^{114}Te, for which three rotational bands have been observed [7], as a representative example in this mass region, using for the first time the same analysis technique developed for the study of rare-earth nuclei. Keeping the above picture in mind we focus mainly on a comparative analysis of the ^{114}Te nucleus with the rare-earth nucleus ^{164}Yb, which is stable in deformation and well studied by discrete line spectroscopy [8].

The fusion reaction ^{64}Ni + ^{54}Cr $\Rightarrow$ ^{118}Te at bombarding energies $E_{\text{beam}} = 230$, 240, 250, 260, and 270 MeV was used. The largest fraction of the data was taken at $E_{\text{beam}} = 250$ MeV which populated the residual nucleus ^{114}Te at the $\approx$20% level. The experiment was carried out

 0031-9007/99/83(25)/5234(4)$15.00

using the tandem accelerator of the Laboratori Nazionali di Legnaro (Italy) and the multidetector array EUROBALL [9]. Data were obtained for a self-supporting thin target with a thickness of 550 μg/cm^2 and for a target 400 μg/cm^2 thick with an Au backing of 50 mg/cm^2. The initial velocity of the residual nuclei in the middle of the target was calculated to be $v/c = 4.6\%$. Energy-dependent time gates on the Ge time signal were used to suppress the background from neutrons. The data for the nucleus ^{164}Yb, which are discussed in comparison with the ^{114}Te data, were obtained in a previous measurement made with the array EUROGAM II [10] using the reaction ^{30}Si + ^{138}Ba at bombarding energies of 140, 145, 150, and 155 MeV. The maximum angular momentum for the Te case was calculated by the Winther model [11] including the collective degree of freedom in the fusion process to be 56$\hbar$, 61$\hbar$, 67$\hbar$, 71$\hbar$, and 74$\hbar$, respectively. For the Yb case the corresponding values of the maximum angular momenta are calculated to be 54$\hbar$, 59$\hbar$, 64$\hbar$, and 68$\hbar$.

In Fig. 1a the spectra obtained at the different bombarding energies gated by the low spin transitions at 709, 775, 734, and 781 keV of ^{114}Te are shown. The spectra have been normalized to the counts associated with the measured average folds at each bombarding energy and corrected for the detection efficiency. The same type of spectra is displayed in Fig. 1b for ^{164}Yb. For the nucleus ^{114}Te a continuous distribution, increasing in intensity with bombarding energy (spin), is seen at $E_\gamma > 1.4$ MeV. This behavior is also observed (at $E_\gamma > 1$ MeV) for ^{164}Yb, which is already known to be a good rotor at low spin and low internal energy. In addition, the energy of the unresolved γ transitions is higher in the case of ^{114}Te as expected for a nucleus with lower mass and value of the moment of inertia. The average energy of the rotational bump moves to higher energy with increasing bombarding energy and maximum angular momentum, which is a typical feature of rotational nuclei. This can be clearly seen in the spectra of both ^{114}Te and ^{164}Yb when constructed as a difference between spectra corresponding to two consecutive bombarding energies, shown in Figs. 1c and 1d, respectively. In addition, values of the fractional Doppler shifts for the edge of the rotational bump measured in forward and backward angles have been obtained using the same type of analysis carried out in Ref. [12]. The values show that the transitions at the edge are fully shifted, thus supporting the strong collective character of the thermal rotation. In the case of ^{114}Te produced at the bombarding energy of 270 MeV, one can clearly note that the measured yield in the continuous bump does not further increase, as shown in Fig. 1a in which the spectra at 260 and 270 MeV almost completely overlap. This fact supports the rotational nature of the continuous bump. One expects to see an energy increase of a rotational bump only up to transition energies corresponding to the maximum value of the angular momentum that the nucleus can sustain. At 260 MeV the limit is reached, and the additional 10 MeV only pumps more energy into the compound nucleus.

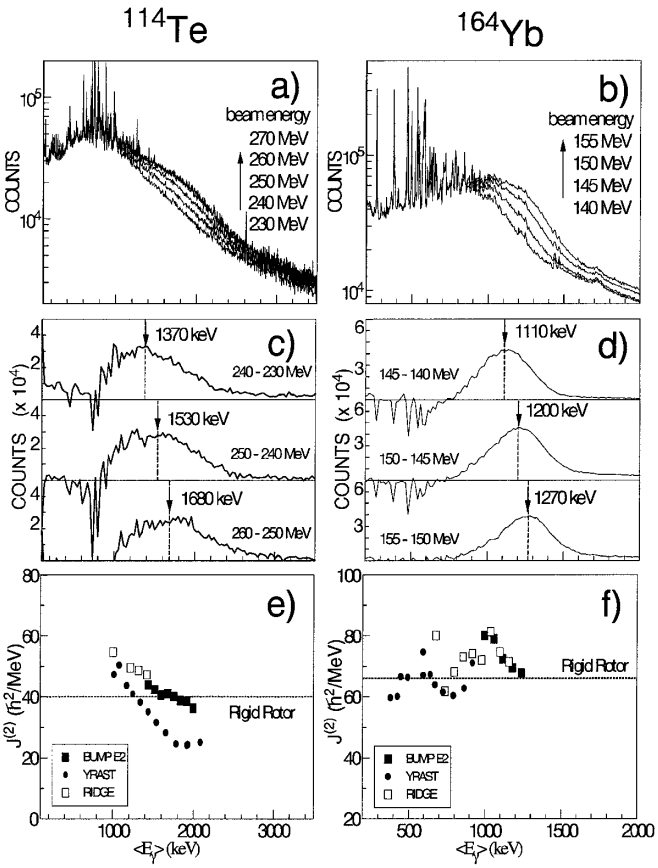

FIG. 1. (a),(b) γ spectra measured at different bombarding energies for ^{114}Te (a) and ^{164}Yb (b). The arrows indicate that the spectra with the lowest number of counts in the continuous distribution correspond to the lowest bombarding energy. (c),(d) Differences between two consecutive bombarding energies. The arrows indicate the positions of the centroids of the distributions. (e),(f) The dynamical moment of inertia $\Im^{(2)}_{\text{eff}}$ for ^{114}Te and ^{164}Yb.

From the measured one-dimensional spectra the value of the dynamical moment of inertia $\Im^{(2)}_{\text{eff}}$ was deduced making use of the relation $H(E_\gamma)/f(E_\gamma) = \Im^{(2)}_{\text{eff}}/4\hbar^2$ discussed in [13,14]. In this expression, $H(E_\gamma)$ is the number of $E2$ transitions at E_γ in the spectrum normalized to the number of counts in the transition connecting the 2^+ to the 0^+ state and corrected for the feeding $f(E_\gamma)$. The results for the $\Im^{(2)}_{\text{eff}}$ of ^{114}Te are shown in Fig. 1e (filled squares) together with the averaged values obtained from the discrete transitions (filled circles) of the known rotational bands [7]. The moment of inertia of the damped transitions of the rotational bump is almost constant and has a value very close to that of the rigid rotor (shown in Fig. 1e with the dashed line). This is in contrast to the behavior of the near-yrast bands, for which the moment of inertia decreases with increasing spin, indicating that the collective rotation terminates (smooth band termination [15]).

The quantity $\Im^{(2)}_{\text{eff}}$ extracted from the quasicontinuum states is an effective moment of inertia, implying that the $E2$ decay paths can proceed in average along an envelope

of bands with different configurations. For ^{114}Te the pronounced decrease in the $\Im^{(2)}_{\text{band}}$, known for the individual bands in this mass region, appears to be washed out; thus the $\Im^{(2)}_{\text{eff}}$ reflects the decay paths rather than intraband transitions [13]. Values of $\Im^{(2)}_{\text{band}} \approx \frac{2}{3}\,\Im^{(2)}_{\text{eff}}$ indicate that one-third of the angular momentum is gained by the alignment of single-particle angular momentum, and two-thirds is gained by collective rotation. In the case of ^{164}Yb (shown in Fig. 1f) the phenomenon of band termination does not take place in the studied spin interval, and consequently the moments of inertia associated with near-yrast bands and with damped transitions show much more similar values and are rather constant with spin. The increase of $\Im^{(2)}_{\text{eff}}$ at about 1 MeV may be caused by the intruding $\pi i_{13/2}$ at higher excitation energy and high spin.

A better identification of the rotational pattern for unresolved transitions can be achieved by examining $E_{\gamma_1} \times E_{\gamma_2}$ coincidence spectra. Systematic studies in the rare-earth region have revealed that the unresolved transitions of regular rotational bands form ridges parallel to the $E_{\gamma 1} = E_{\gamma 2}$ diagonal valley, while damped transitions from the mixed rotational bands fill the valley region. The Te data were sorted in a $E_{\gamma 1} \times E_{\gamma 2}$ spectrum gated by the same low lying transitions of ^{114}Te used for the one-dimensional analysis. The Compton and other uncorrelated events were reduced by employing the standard background subtraction treatment, named COR, described in Ref. [16]. The contribution of the known intense discrete transitions was fitted and removed by means of Radware programs [17]. In Figs. 2a and 2b, two perpendicular cuts, 100 keV wide at $\langle E_\gamma \rangle = 0.5(E_{\gamma 1} + E_{\gamma 2}) = 1200$ and 1400 keV projected onto the axis $E_{\gamma 1} - E_{\gamma 2}$, are displayed. In Figs. 2c and 2d, similar spectra for ^{164}Yb (with cuts 60 keV wide at $\langle E_\gamma \rangle = 920$ and 1040 keV) are shown for comparison. The well-known ridge-valley structure is clearly seen in the case of ^{164}Yb, and can also be recognized in the ^{114}Te case although it is less pronounced with wider ridges. It is also clearly seen that the separation between the inner ridges is larger for ^{114}Te than for ^{164}Yb, as a consequence of the rotation of a nucleus with a smaller moment of inertia. The energy difference for two rotational ridges equal to $8/\Im$ was used to obtain the values of the dynamical moment of inertia. The corresponding results, shown with open squares in Figs. 1e and 1f, are somewhat larger than obtained for the yrast states.

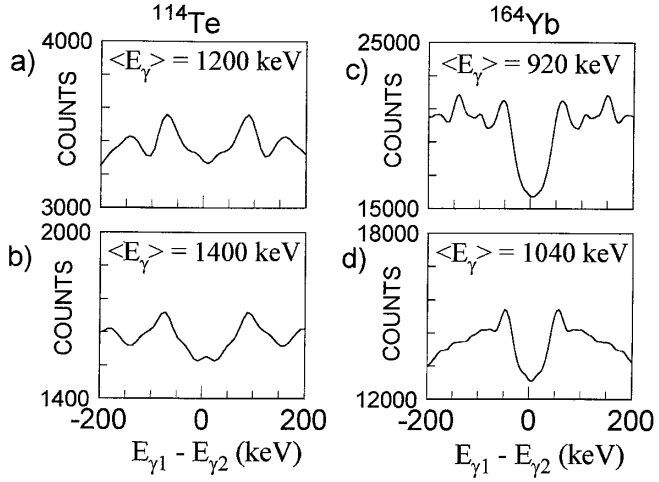

FIG. 2. Perpendicular cuts on the $E_{\gamma_1} \times E_{\gamma_2}$ matrices for ^{114}Te [(a),(b)] and ^{164}Yb [(c),(d)] for two different values of $\langle E_\gamma \rangle$.

The $E_{\gamma 1} \times E_{\gamma 2}$ spectrum was analyzed using the fluctuation analysis technique [3], developed to extract quantitative information from the quasicontinuum spectra. The finiteness of counts in each individual cascade leads to fluctuations in the spectrum superimposed on the ordinary statistical fluctuations in the number of counts. In particular, the number of paths available to the nucleus in the different decay modes can be obtained from the data. The number of two step pathways, $N^{(2)}_{\text{path}}$, may be extracted by selecting intervals in the spectrum, corresponding to one pair of transition per cascade in average, from squares of $(4/\Im_{\text{eff}}) \times (4/\Im_{\text{eff}})$ keV^2 in the valley or along the ridges [3].

In Fig. 3a the results obtained from the analysis of the ridges in ^{114}Te are shown in comparison with the ^{164}Yb data. In the case of ^{114}Te, because of the complex level scheme with high energy transitions at low spin, the number of clean cuts for which the fluctuation analysis could be applied is more limited than for ^{164}Yb. The number of paths deduced from the ^{114}Te data is found to be, on average, approximately a factor of 2 smaller than that of ^{164}Yb.

The theoretical $N^{(2)}_{\text{path}}$ can be extracted by counting the number of two consecutive transitions for which the

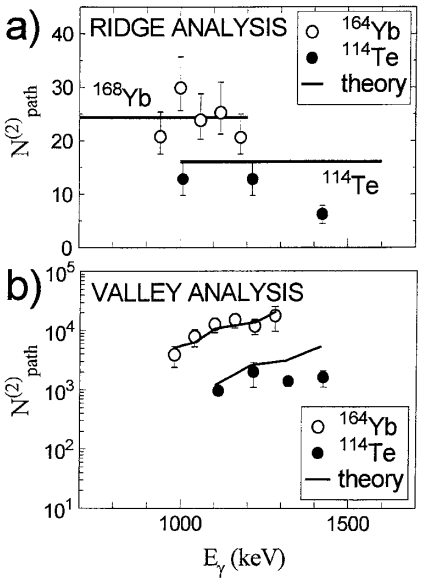

FIG. 3. (a) The quantity $N^{(2)}_{\text{path}}$ obtained with the fluctuation analysis of the measured first ridges of ^{114}Te and ^{164}Yb, in comparison with the theoretical results (solid lines). (b) The quantity $N^{(2)}_{\text{path}}$ extracted from the valley analysis for ^{114}Te and ^{164}Yb, in comparison with the theoretical results for ^{168}Yb and ^{114}Te (solid lines).

corresponding branching number $n_{\mathrm{branch}}(i) = (\sum_j S_{i,j}^2)^{-1}$, where $S_{i,j}$ is the normalized strength from level i at spin I to level j at spin I-2, is less than or equal to 2. The values obtained for the band mixing calculations [1], averaged over the spin interval $(25-35)\hbar$, are shown for ^{114}Te and ^{168}Yb with the solid lines in Fig. 3a in comparison with the data on $N_{\mathrm{path}}^{(2)}$ from the ridge structure. In the case of the ^{164}Yb data the comparison is made with the available calculations for ^{168}Yb which describe the average features of the quasicontinuum of rare-earth nuclei (cf. [10] and [12]).

The number of paths obtained from the analysis of the valley region, collecting mostly damped transitions from states at which one expects the fragmentation of the rotational decay, is shown in Fig. 3b. Also, in this case, a significant difference is seen between the results of ^{114}Te and ^{164}Yb data. The expected values of $N_{\mathrm{path}}^{(2)}$ based on the same band mixed calculations used for the ridge analysis are shown by the solid lines in Fig. 3b. These predicted values were obtained by applying the fluctuation analysis technique to a simulated spectrum based on the calculated levels and transition probabilities (cf., e.g., Ref. [18]). The calculations are found to reproduce both the ridge and the valley results quite well.

Altogether, the present experimental results show that γ cascades of thermally excited deformed nuclei are governed by damped rotational motion, not just for rare-earth nuclei but also for the lighter ^{114}Te nucleus. The quantitative agreement between calculations and experiment in Fig. 3 strongly supports the scaling with mass number of the residual interaction and the level density. According to the present calculation, damping should set in at about heat energy $U_0 \approx 0.9-1.0$ MeV in ^{114}Te, compared to $U_0 \approx 0.7-0.8$ MeV in ^{164}Yb. The values of the damping widths predicted by the band mixing calculations are approximately a factor of 2 larger for ^{114}Te than for ^{168}Yb. The number of paths in the valley cannot by itself support the predicted scaling for the damping width because it depends quadratically on Γ_{rot} but more strongly on the level density. However, an upper limit for Γ_{rot} is inferred from the value of the measured width of the difference spectra shown in Figs. 1c and 1d. In the present case this width is found to be larger by a factor of $\approx$2 in the case of ^{114}Te (with values 800–1000 keV) as compared to that of ^{164}Yb (with values 300–400 keV), supporting the scaling of Γ_{rot} with mass number and displaying an internal consistency in the analysis.

In summary, there are two relevant conclusions obtained in this paper. The first is that the study of the mass dependence of the rotational damping process has provided a stringent test for effects beyond mean field, which are found in this case to be rather well described by the existing model. The second is that the fluctuation analysis method is indeed a powerful tool for obtaining valuable physical information from continuum spectra.

The work has been supported by the Italian Istituto Nazionale di Fisica Nucleare and the Danish Natural Science Research Council.

[1] M. Matsuo *et al.*, Nucl. Phys. **A617**, 1 (1997); Nucl. Phys. **A649**, 379c (1999).
[2] B. Lauritzen, T. Døssing, and R. A. Broglia, Nucl. Phys. **A457**, 61 (1986).
[3] T. Døssing *et al.*, Phys. Rep. **268**, 1 (1996).
[4] S. Leoni *et al.*, Nucl. Phys. **A587**, 513 (1995).
[5] R. A. Broglia *et al.*, Phys. Rev. Lett. **58**, 326 (1987).
[6] M. A. Deleplanque *et al.*, Phys. Rev. Lett. **41**, 1105 (1978).
[7] I. Thorslund *et al.*, Phys. Rev. C **52**, R2839 (1995).
[8] A. Norlund *et al.*, Nucl. Phys. **A591**, 117 (1995).
[9] J. Simpson, Heavy Ion Phys. **6**, 253 (1997).
[10] S. Frattini *et al.*, Phys. Rev. Lett. **81**, 2659 (1998).
[11] A. Winther, Nucl. Phys. **A594**, 203 (1995).
[12] B. Million *et al.*, Phys. Lett. B **415**, 321 (1997).
[13] F. S. Stephens, Phys. Scr. **T5**, 5 (1983).
[14] M. A. Deleplanque *et al.*, Phys. Rev. Lett. **50**, 409 (1983).
[15] I. Ragnarsson *et al.*, Phys. Rev. Lett. **74**, 3935 (1995).
[16] O. Andersen *et al.*, Phys. Rev. Lett. **43**, 687 (1979).
[17] D. C. Radford, Nucl. Instrum. Methods Phys. Res., Sect. A **361**, 297 (1995).
[18] A. Bracco *et al.*, Phys. Rev. Lett. **76**, 4484 (1996).